Ecological Modelling 418 (2020) 108908

Contents lists available at ScienceDirect

Ecological Modelling

journal homepage: www.elsevier.com/locate/ecolmodel

Changes in upwelling regimes in a Mediterranean-type lagoon: A model application

L. Aveytua-Alcazar[a], D. Melaku Canu[a,*], V.F. Camacho-Ibar[b], C. Solidoro[a]

[a] Istituto Nazionale di Oceanografia e di Geofisica Sperimentale, Borgo Grotta Gigante 42/C, 34010, Sgonico, Trieste, Italy
[b] Universidad Autónoma de Baja California, Instituto de Investigaciones Oceanológicas, Carretera Transpeninsular Ensenada-Tijuana No, 3917, Frac. Playitas, Ensenada, B.C, 22860, México

ARTICLE INFO

Keywords:
Nitrogen
Modelling
Coastal lagoon
Upwelling regimes
SHYFEM
SQBFEEM

ABSTRACT

San Quintín Bay (SQB) is a coastal lagoon fertilized with cold, nutrient rich, marine water, that sustains the high productivity within the bay, in particular during upwelling events. The variations in the oceanic exchanges -and in particular changes in upwelling intensity and frequency, also related to climate change- are expected to alter the biogeochemical processes in SQB and in the other coastal systems along the California Current domain with possible impacts on the trophic state. The extent of this influence is tested here developing and applying a 3-D coupled physical-ecological model (SHYFEM-SQBFEEM), contrasted with data. Simulations included a reference scenario (REF) of typical upwelling conditions, observed in spring 2004, and two scenarios of low (LOW) and high (HIGH) upwelling conditions, observed, respectively during spring 2016 and 2005. We calculated the N-budget for the three scenarios, highlighting the response of primary and secondary producers, including oyster potential production, to the changes in upwelling intensity. The model shows that upwelling intensity has a large influence on N availability and consumption within the bay, and on the response of primary and secondary producers. Differences of the nitrogen stocks of primary and secondary producers under HIGH and LOW upwelling conditions are of around 25 % for phytoplankton, 20 % for oyster and more than 40 % for zooplankton.

1. Introduction

Eastern Boundary Upwelling Systems (EBUS) are biologically productive marine regions covering < 1 % of the ocean area, but providing up to 20 % of the world's capture fisheries (see references in García-Reyes et al., 2015). These systems (i.e. California, Humboldt, Canary/Iberian and Benguela Currents) provide ecosystem, economic and recreational services to people living along their coasts and in their immediate hinterlands (García-Reyes et al., 2015).

Ecosystem productivity in coastal upwelling systems, along with the goods and services they provide is threatened by global climate change (Bakun et al., 2015). Although the driving mechanism is still being actively debated, previous studies appear to consistently predict that the upwelling in EBUS has intensified and that the increasing trend will continue (Bakun et al., 2015; Xiu et al., 2018). Recent studies have suggested that the timing of upwelling has trended toward delayed and shorter upwelling seasons in the northern portion of the California Current System (CCS) and longer upwelling seasons in the southern portion (García-Reyes et al., 2015). Ibarra-Obando et al. (2001) reported that the variability of biogeochemical dynamics in the southern region of the CCS, along the Baja California Peninsula, might change from year to year depending on inter-annual processes such as "El Niño" phenomenon, during which changes occur such as the reduction in nutrient concentration and the delay of phytoplankton blooms.

Variability in the biogeochemical properties of upwelled waters will influence the ecology and productivity in coastal systems. During upwelling events, which are particularly strong in the CCS in spring and summer, nutrient-rich shelf waters are transported by tidal advection into adjacent semi-enclosed coastal ecosystems, supplying dissolved inorganic nutrients (Hickey and Banas, 2003; Brown and Ozretich, 2009). During relaxation periods, after upwelling events, shelf waters may also supply upwelling-generated phytoplankton (Banas et al., 2007). Once the upwelling generated phytoplankton goes through remineralization, it becomes an additional indirect source of nutrients for the estuarine primary producers (Camacho-Ibar et al., 2003), and an additional energy source for the estuarine secondary producers, including commercially produced species (Ruesink et al., 2003; Banas et al., 2007). Oceanic nutrient supply can be the most significant source of nutrients during the upwelling season in the NE Pacific coast estuaries (e.g., Willapa Bay, Yaquina Bay, Tillamook Bay and Tomales Bay),

* Corresponding author.
E-mail address: dcanu@inogs.it (D. Melaku Canu).

https://doi.org/10.1016/j.ecolmodel.2019.108908
Received 17 September 2019; Received in revised form 28 November 2019; Accepted 29 November 2019
Available online 07 January 2020

where terrestrial supply of nutrients occurs throughout the year (Chapin et al., 2004; Hickey and Banas, 2003; Brown and Ozretich, 2009; Colbert and McManus, 2003; Smith and Hollibaugh, 1997). Upwelling is the main source of nutrient supply for the Baja California coastal lagoons, located in the southern region of the California Current domain, (e.g., San Quintín Bay, Ojo de Liebre Lagoon, and Magdalena Bay) that receive intermittent terrigenous supply, as streams are completely dry except during heavy rains (Ibarra-Obando et al., 2001). These systems are highly productive (Ibarra-Obando et al., 2001) and strongly rely on nutrient supply from the ocean not only during the season of upwelling intensification but throughout the year, probably through the internal recycling of nutrients when upwelling is at its minimum or absent.

Even though EBUS have been extensively studied for nearly a century and there is a vast body of literature examining climate impacts on upwelling ecosystems (García-Reyes et al., 2015; Xiu et al., 2018), studies addressing the impact of climate change on coastal lagoons and estuaries are scarce.

Models are useful tools to address the pressing question of how natural systems will respond to future changes in climate (Chavez, 2012). Physical-biogeochemical models have been used in CCS to understand the links between upwelling intensity and physical forcing (wind and circulation variability) (Fiechter et al., 2018). Arellano and Rivas (2019) recently investigated the response of coastal upwelling to climate in CCS, along the western coast of the Baja California Peninsula, by modeling the effect of the variation in surface warming (that increases the stratification of the water column) and intensification of coastal alongshore winds.

Previous model applications in the CCS also highlight the ecosystem sensitivity to changes in the onset of upwelling spring transition. An early spring transition resulted in increasing vertical nutrient flux at the coast, that propagates spatially and through the food web (Chenillat et al., 2013).

The objective of the present study is to assess the response of different upwelling regimes in San Quintin Bay (SQB), a coastal lagoon located in the CCS, on the northwest coast of Baja California Peninsula, Mexico. Our understanding of local feedbacks between local biological production and biogeochemical properties of upwelling waters in coastal systems is scarce, and needs to be addressed in order to highlight the possible impacts on the ecology and socio-economic components at the local level.

Site-specific high resolution models are needed to address the specificity of restricted and shallow water environments. Previous model applications in SQB focused on the 2-D water circulation (Melaku Canu et al., 2016) and on the biogeochemistry, exploring the upwelling effect in 1-D (Aveytua-Alcazar et al., 2008), but a fully coupled hydrodynamic-biogeochemical model was missing.

Here we explored the spatial/temporal variability of the trophic properties of the bay, computing the nutrient stocks and nutrient fluxes among the components of the lower trophic web. In order to perform this analysis, we adapted a finite element ecological model, which was originally developed for the lagoon of Venice (the Venice Lagoon Finite Element Ecological Model, VELFEEM, Umgiesser et al., 2003; Melaku Canu et al., 2001, 2003) by integrating an ecological-water quality module and a fine element 3-D hydrodynamic model based (Shallow Water Hydrodynamic Finite Element Model, SHYFEM, Umgiesser et al., 2004). More in detail, in order to capture relevant trophic features of the SQB here we added new modules to VELFEEM for simulation of the hereafter called SQBFEEM (San Quintin Bay Finite Element Ecological Model).

2. Study area

San Quintin Bay is a coastal lagoon of Mediterranean type (Largier et al., 1997) located in the CCS, on the northwest coast of the Baja California Peninsula, Mexico (30°27′N and 116°00′W; Fig. 1). SQB is a moderately hypersaline system throughout the year (Camacho-Ibar et al., 2003 and 2007), with salinity levels increasing from the ocean inlet toward the inner regions. This lagoon is Y-shaped and covers an area of approximately 42 km^2, with an eastern arm known as Brazo San Quintin (brazo SQ) and a western arm known as Bahia Falsa (BFa). Narrow channels running in the bay have a maximum depth of 5–15 m, while the rest of the area has an average depth of 2 m. This temperate region of the Baja California Peninsula has a mean annual precipitation of 150 mm and a mean annual evaporation of 1400 mm; rainfall is restricted to the period of November-March (Aguirre-Muñoz et al., 2001). Inputs of water and other terrigenous materials from the San Simon stream to the lagoon only occur in years of above-average rainfall. Most of the inhabitants of the catchment, which is a rural area, live away from the SQB. Tourism is one of the main economic activities in the area but it is still limited and represents a minor indirect source of nutrients to the bay. An important economic activity in SQB is aquaculture of the Pacific oyster *Crassostrea gigas*. This activity is restricted by regulation to BFa (Fig. 1), where it presently covers around the 300 ha of the shoal areas (˜7 % of the total bay area), and represents a relevant export of organic production, therefore of nutrients, from SQB.

Camacho-Ibar et al. (2003) pointed out that SQB is a net sink of phytoplankton imported from the ocean, in particular during the upwelling periods (Farfán and Álvarez-Borrego, 1983). Phytoplankton in SQB typically decreases from the mouth toward the inner arms of the lagoon, and during the intense upwelling season, the phytoplankton community composition is very dynamic, with diatoms dominating early in an upwelling event and dinoflagellates dominating after the diatom bloom (Millan-Nuñez et al., 1982; Gracia-Escobar et al., 2014).

The dominant primary producers, apart from microalgae, include the seagrass Zostera *marina* and the macroalgae *Ulva spp*. (Zertuche-González et al., 2009). The eelgrass covers ˜40 % of the lagoon and forms particularly dense meadows in the inner arms (Ward et al., 2003). Ibarra-Obando et al. (2007) reported an average annual foliar biomass of *Zostera marina* in SQB of 75 g DW m^{-2}, with annual maxima ranging from ˜80 to ˜350 g DW m^{-2}, and an average in the summer-autumn maxima of ˜150 g DW m^{-2}. *Ulva spp*. is present all year around, but its biomass shows a seasonal variation with a spring maximum (Ward et al., 2003). Zertuche-González et al. (2009) reported biomasses of ˜350 g DW m^{-2} of *Ulva spp.* in SQB in spring-summer 2004 and 2005, and ˜65 g DW m^{-2} in late winter 2005. *Ulvaspp.* biomass has increased in recent years (Zertuche-González et al., 2009), competing with *Zostera marina*, in particular close to the SQB inlet (Ward et al., 2003).

3. Materials and methods

3.1. The model implementation in the San Quintin Bay

The water quality model, hereon called SQBFEEM (Finite Element Ecological Model for the San Quintin Bay) has been developed coupling the finite element hydrodynamical model, already successfully applied to the SQB in a 2D version (Melaku Canu et al., 2016), to a biogeochemical model, by significantly expanding the work already made in VEELFEM (the Finite Element Ecological Model for the Lagoon of Venice, Umgiesser et al., 2003; Melaku Canu et al., 2003) in order to incorporate major ecological processes that were not included in VELFEEM, but are needed for a proper representation of the SQB biogeochemistry. In particular, we added three new modules for Nitrogen (N), Carbon (C) and Phosphorus (P) cycling through macroalgal mats, oyster culture farms, and the detritus stock in the sediment.

Following the VELFEEM approach we used an operator splitting technique, as described in Umgiesser et al. (2003). Accordingly, the overall variation of any state variable is split into the sum of two contributions: the physical driven term and the biological driven term. The hydrodynamic model resolves the momentum and continuity equation to update the current velocities and water levels, then the

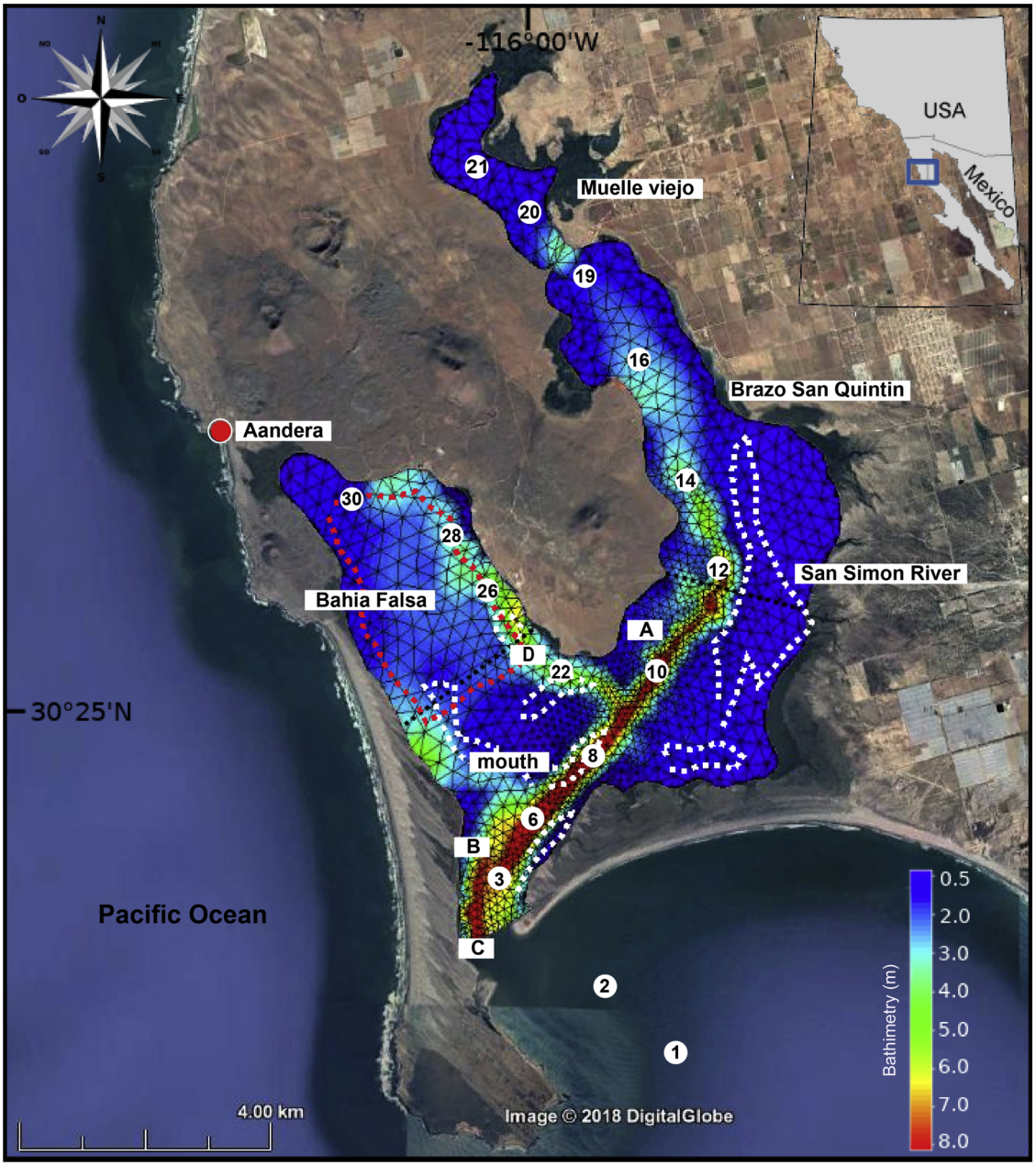

Fig. 1. Map of San Quintin Bay (SQB) with bathymetry and model grid. Numbers (1–30) indicate sampling stations. The location of the ADCPs (A, C, D), the oceanographic buoy (B), and the meteorological station (Aandera). The red and white dots pattern show the areas, where the oyster cultured farms and macroalgal mats are respectively located. (For interpretation of the references to colour in this figure legend, the reader is referred to the web version of this article).

physical (temperature and salinity) and biogeochemical variables (i.e. nutrients, phytoplankton, zooplankton, detritus) are transported (advected and diffused). All the variables (including Ulva and oysters which are not transported) are then updated performing biogeochemical and ecological transformations.

The SHYFEM model uses a finite element discretization to solve the hydrodynamic equations and a semi-implicit time-stepping algorithm and therefore it is suitable for the hydrodynamic characterization of shallow basins with a complex morphology, including channels and tidal flats (Umgiesser et al., 2003, 2004, 2014; Melaku Canu et al., 2003, 2012, Solidoro et al., 2004). Adopting a staggered approach, the water levels are described by linear form functions defined on the nodes (intersections) of the grid, while the velocities are described by constant form functions over each element, which corresponds to the definition of the velocities in the centre of the elements (Umgiesser et al., 2004). The SQB domain has been represented by a finite element grid made of 1481 nodes (vertices) and 2633 triangular elements varying in shape and dimension, from 7 m along the channels and at the inlet to 35 m in the shallower areas (Fig. 1) (Melaku Canu et al., 2016). The water column is discretized into 8 vertical layers, with uniform thickness of 2 m.

The SQBFEEM model follows the evolution of a set of variables which characterize the state of the water column and of the surface of sediments, which hosts the benthic communities. The state of the water and sediment is defined by: ammonium (NH_4), nitrate (NO_3), phosphate (PO_4), dissolved organic nitrogen (DON), particulate organic nitrogen (PON), dissolved organic phosphorus (DOP), particulate organic phosphorus (POP), carbonaceous biogeochemical oxygen demand (CBOD), dissolved oxygen (DO), phytoplankton, zooplankton, *Crassostrea gigas* and *Ulva spp* (Fig. 2). In the present work, the model is refined by introducing a sedimentation module, representing the dynamics of organic matter that settles from the water column to the bottom layer

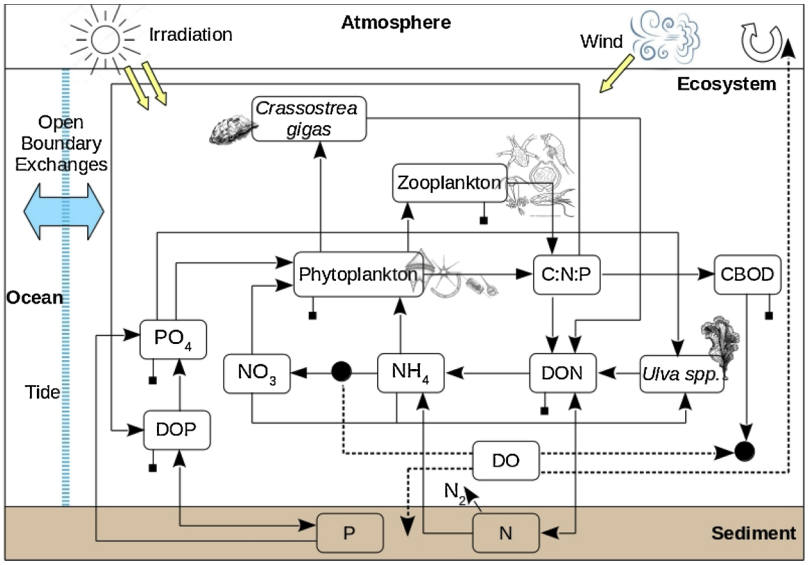

Fig. 2. Conceptual model of the biological and physical interactions between the components used in the SQBFEEM. Arrows indicate the matter flow between the state variables. The dashed lines indicate the dissolved oxygen fluxes.

where it is mineralised and, eventually, resuspended. The inclusion of these processes into the parameterization of biogeochemical cycles is of great importance, since this bay is a shallow environment and both re-suspension of sediment and release of nutrients from the sediment can be high, and significantly affect the water quality (Aveytua-Alcázar et al., 2008; Ávila-López et al., 2016).

The limiting factors are computed following the standard formulations: the Michaelis Menten-Monod for nutrient limitation, the Steele formulation for the limitation due to light intensity, and an exponential relation for temperature.

Since oyster aquaculture of *Crassostrea gigas* may significantly contribute to the nutrient dynamics in the SQB ecosystem (Sandoval-Gil et al., 2016), the new module representing the oysters stock has been introduced (Fig. 2). Individual filtration, assimilation, excretion and ingestion, were introduced as functions of body size, temperature and food quantity (Solidoro et al., 2000; Chapelle et al., 2000; Pastres et al., 2001; Melaku Canu et al., 2011). The model was initialized introducing the 25 in./m^{-2} of an average size of 20 mm distributed across BFa (Fig. 1), and introducing a growth term, and an exponential death rate.

According to Zertuche-González et al. (2009) *Ulva spp*. became quite invasive in the last decade in SQB, having also replaced extensive surfaces of eelgrass beds. Its presence was hypothesized to have been triggered by the introduction of oyster cultivations. According to the same authors, Ulva may play an important role as temporary sink and source of C, N, and P in SQB due to its large biomass and to its capacity to capture these elements, and to release them during the degradation phase (Ávila-López et al., 2017).

Aveytua-Alcázar et al. (2008) report that NO_3 concentrations in the water column are more sensitive to Ulva variations than Zostera in SQB. On the other hand, the temporal variability of *Zostera marina* biomass is more sensitive to light availability than NO_3, and *Ulva spp*. is more sensitive to NO_3 availability than light. This suggests that it is more important to included Ulva in our model. Therefore, we introduced a new *Ulva spp.* module (Fig. 2) dynamically simulating the temporal evolution of biomass and of the intratissual N in *Ulva spp*., based on the formulations given in Solidoro et al. (1997). The module parameterization is listed in Table A1.

The model results have been statistically tested by calculating an index of performance (Allen et al., 2007) which takes into account the explained variance (R^2), the Nash-Sutcliffe Model Efficiency (ME), the percentage bias model (Pbias), and the ratio between the standard deviation of the data and the standard deviation of the model (RSD). The index of performance identifies 4 levels, which are categorized as excellent (ME > 0.65, Pbias < 10), very good, (ME: 0.65-0.5, Pbias: 10–20), good (ME: 0.5–0.2, Pbias: 20–40) and poor (ME < 0.2, Pbias > 40).

3.2. Model set-up

A 1-year run, with a time step of 5 min, was performed for 2004, in order to test the model and to tune the model parameters. In addition, in order to explore the effect of variation in upwelling intensity on the SQB biogeochemistry, we performed two additional runs for two years, 2005 and 2016 characterized, respectively, by intense (high) and weak (low) upwelling conditions. We therefore focused the comparative analysis on the effects of upwelling changes on the N budget of SQB in spring, when the upwelling intensification occurs. These three years were selected based on nutrient data availability, and on the availability of hydrological parameters (wind speed, seawater temperature and salinity); the magnitude of the coastal upwelling indices (CUI), calculated by NOAA as the magnitude of the offshore transport component, normal to the coastline orientation (m^3 s^{-1} /100 m of coastal line) (https://www.pfeg.noaa.gov/products/PFEL/modeled/indices/upwelling/upwelling.html) was also considered. CUI calculated at the point 30°N, 119°W is respectively 94, 110 and 71 m^3 s^{-1} /100 m of coastal line, for the spring upwelling periods of 2004, 2005 and 2016 (Table 1).

A scenario analysis on the different spring upwelling intensity conditions of REF (2004), LOW (2016) and HIGH (2005) was performed.

3.3. Meteorological forcing, boundary conditions and initial conditions for the REF, LOW and HIGH scenario simulations

The 3-D hydrodynamic model was forced with hourly observations of wind speed, air temperature, air humidity, irradiance and atmospheric pressure sampled at the Aandera Weather Station located at the northeastern end of BFa (Fig. 1). Model setup (boundary and forcing data) for the REF, LOW and HIGH scenarios are listed in the Table 2.

3.3.1. The reference scenario (REF)

The REF scenario, for the year 2004, was set adopting the hydrodynamic- thermohaline setup in agreement with Melaku Canu et al. (2016), and the biogeochemical set-up in agreement with Aveytua-

Table 1
Average values of hydrological observations in SQB (wind speed, seawater temperature and salinity), and the upwelling index (m3 s^{-1} / 100 m of coastline) under the three upwelling conditions (REF, LOW and HIGH).

Data	Upwelling Index ($m^3 s^{-1}$/100 m^{-1})	Wind Speed ($m^2 s^{-1}$)	Temperature (°C)	Salinity
REF April-June 04	94	3.05 ± 2.03	15.0	33.3
HIGH April-June 05	110	4.30 ± 2.02	14.0	33.8
LOW April-June 16	71	2.10 ± 1.38	16.5	34.0

Alcázar et al. (2008). In the spring campaign, the average wind speed (4.18 ± 1.64 m s^{-1}) revealed intense and intermittent upwelling winds in the first days (22–30 May), and weak upwelling winds (3.39 ± 2.06 m s^{-1}) in the last days (15–25 Jun). In the 9 first days upwelling was intense but intermittent, CUI was highest (> 100 m^3 s^{-1} /100 m of coastal line), in the following days upwelling was weak and CUI was ˜50 m^3 s^{-1} /100 m of coastal line. The average wind speed in summer of 2004 (3.04 ± 1.84 m s^{-1}) was less intense than the spring campaign of the same year (Table 1).

3.3.1.1. REF-Boundary conditions. Open ocean boundary conditions were set using sea level, seawater temperature and salinity values measured at the SQB mouth at station C (Fig. 1). Sea level values collected at 30 min intervals were measured using a RDI acoustic Doppler current profiler. Because a one-year-long time series of nutrients is not available for SQB, nutrient boundary conditions were obtained by using data measured at stations 1 and 2 (Fig. 1) in May-June and September-October 2004 and with monthly measurements of Pennington and Chavez (2000). Data were interpolated following a seasonal upwelling. Zooplankton boundary conditions were set using the IMECOCAL data (http://calcofi.org/affiliates/228-aer-imecocal.html) measured at the ocean station nearest SQB.

3.3.1.2. REF-Initial conditions. nutrients, phytoplankton and zooplankton values were set in agreement with experimental values for the year 2004 given in Aveytua-Alcázar et al. (2008). Due to the lack of data of nutrients in SQB throughout the whole year, winter nutrient concentrations were set at the mid-intensity upwelling observed values (4 μM for NO_3, 4 μM for NH_4, 1 μM for PO_4). The initial biomass of *Ulva spp*. was set to 40 gDW m^{-2}, distributed across an area of 431 ha (Fig. 1), in agreement with reported observations (Zertuche et al., 2009; Aveytua-Alcázar et al., 2008). The oyster module was initialized in agreement with García-Esquivel et al. (2004).

3.3.2. The High-Upwelling scenario (HIGH)

The HIGH scenario was based on hydrodynamic, thermohaline and biogeochemical setting for 2005 (Aveytua-Alcázar et al., 2008; Ribas-Ribas et al., 2011) and on 2005 data of wind speed, air temperature, humidity, irradiance and atmospheric pressure collected at the Aandera Weather Station (Fig. 1). The average wind speed in the spring 2005 was more intense in comparison to REF scenario, with a mean of 4.30 ± 2.02 m s^{-1} (Table 1).

***3.3.2.1*.HIGH-Boundary conditions**: were set using data of 2005 and adopting the same approach applied for the computation of the REF boundary conditions. Sea level, water temperature and salinity values were measured at the SQB mouth at station C (Fig. 1). Concentrations of nutrients, phytoplankton and zooplankton were obtained by using data measured at stations 1 and 2 (Fig. 1) in May-June and adopting the same approach used for the REF setup to extrapolate the year long boundary conditions.

***3.3.2.2*HIGH-Initial conditions:** were set using 2005 data and adopting the same approach applied for the computation of the REF initial conditions.

3.3.3. The Low-upwelling scenario (LOW)

The LOW scenario was set using biogeochemical and hydrodynamic data of the year 2016. The wind speed in the spring 2016 was less intense in comparison with to REF scenario, with a mean of 2.10 ± 1.38 m s^{-1} (Table 1).

***3.3.3.1*LOW-Boundary conditions:** hydrodynamic open ocean boundary conditions were set using tidal height computed using MAR V0.7 (http://oceanografia.cicese.mx/predmar/). Seawater temperature, salinity and Chl-a data were obtained from a buoy equipped with a multiparameter probe (YSI 6920V2–2) anchored at the mouth of the bay (st. B in Fig. 1); recorded at 15-min intervals from January to December 2016. Chla a data were converted to carbon units using the 60 mg of C per mg of Chl-a factor (Parsons et al., 1984). Concentrations of nutrients were set using 2016 data and extrapolations adopting the same approach applied for the computation of the REF boundary conditions. Upwelling in the LOW scenario was less intense in comparison to REF scenario; accordingly, nutrient values were 25 % lower in average.

***3.3.3.2*LOW-Initial conditions:** were set using 2016 data and adopting the same approach applied for the computation of the REF initial conditions.

4. Results and discussion

4.1. The REF scenario, results and comparison with available data

The REF scenario model outputs were compared with i*n situ* observations of water levels (RDI acoustic Doppler current profiler), seawater temperature, salinity and nutrient concentration (Fig. 1) available for 10 days in spring (May-June) and 14 days in summer (September-October) 2004. Physical variables are consistent with those obtained with the validated 2-D model (Melaku Canu et al., 2016). The modeled currents show satisfactory agreement with ADCP data (already presented in Melaku Canu et al., 2016) measured at stations A and D shown in Fig. 1. The coefficient of determination (R^2) is 0.87 and 0.8, respectively, for the two stations A and D. In spring, water temperature and salinity fields presented the expected pattern, with a positive gradient from the mouth toward the internal area, at the heads of BFa and brazo SQ, with a difference of 4 °C for temperature and 0.8 for salinity between these two extremes.

The comparison of modelled and observed vertical profiles, confirms the occurrence of well mixed profiles structure in the Bay. A weak spring vertical structure (less than 10 % of variation) was observed at station 6, close to the mouth of the Bay, which is the deepest part of the system. The mixed vertical structure of the SQB was already reported by other authors (Millan-Nuñez, et al.,1982 and Ribas-Ribas et al., 2011).

As expected, the simulated annual evolution of nutrients (NO_3, NH_4 and PO_4), phytoplankton and zooplankton shows a maximum in late spring and early summer and a minimum in winter and early spring, in accordance with the typical biogeochemical dynamics, governed by upwelling, observed in central California (Chenillat et al., 2013 and Pennington and Chavez, 2000). An example of such annual evolution is shown for station 28 in Fig. 3. Having a residence time of ˜4 days (Melaku Canu et al., 2016), this station is quite rapidly responding to the ocean physical dynamics and nutrient supply, but is still influenced by the local dynamics of oyster, macroalgae and phytoplankton growth, all of which are abundant. During upwelling events, which occur through the year but are more intense during spring and early summer, upwelled water from the CCS is transported from the shelf into SQB; the penetration of upwelled water into the arms varies according to the combination of upwelling intensity and tidal amplitude (Melaku Canu et al., 2016; Ribas-Ribas et al., 2011). The simulations show that, when upwelling events occur, tidal pumping (Fig. 3) induces a large injection of NO_3 into SQB. This induces, in station 28, higher nutrient

Table 2
Description of the boundary, initial and forcing model conditions for the REF, LOW and HIGH scenarios.

Scenario	Boundary Conditions	Initial Conditions	Meteorological forcing
REF	Experimental data at stations 1 and 2, and extrapolated data.	Experimental data of mid-intensity upwelling	Sampling station Aandera
LOW	Experimental data of the buoy equipped and extrapolated data.	Experimental data of mid-intensity upwelling	Sampling station Aandera
HIGH	Experimental data of stations 1 and 2, and extrapolated data.	Experimental data of mid-intensity upwelling	Sampling station Aandera

concentration during the spring tide, when NO_3 reaches maximum values of ˜7 μM, and lower concentration during the neap tide, when the NO_3 maximum reaches only ˜4 μM (Fig. 3).

The spatial and temporal comparison (Fig. 4A, B, C and D) show good agreement between averaged observed and simulated values. The tendency of NO_3 to decrease towards the interior of the lagoon in both seasons (Fig. 4A) indicates that NO_3 is consumed within SQB. NO_3 average values in BFa were slightly lower than at the mouth of

the bay, due to the limited exchange with the ocean, computed with the average water residence times of 4 days.

In brazo SQ, where the average water residence time is ˜11 days, the decrease in NO_3 concentration with respect to the mouth of the bay is even higher, confirming previous results (Camacho-Ibar et al., 2003 and 2007; Ribas-Ribas et al., 2011). PO_4 (Fig. 4D) shows a different pattern than NO_3, increasing from the mouth to the inner parts of the bay, confirming that this system is a net generator of this nutrient as a result of its addition from remineralization of imported organic matter over its consumption by the local primary producers (Camacho-Ibar et al., 2003 and 2007).

In summer, the persistence of NH_4 in the water column which is already depleted in NO_3 (st. 28; Fig. 3), is explained by the remineralization of the organic matter mainly occurring in the sediments. Ibarra-Obando et al. (2004) report that sediments of SQB can provide NH_4 to the water column at rates as high as 2.7 mmol NH_4 $m^{-2}d^{-1}$. As a result of the first step of organic matter degradation, the model reproduces the net increase of DON in the inner parts of SQB (Fig. 4D), in agreement with observations reported by Rodriguez-Cardozo (2004) that found, in the internal arms, average values of DON of 16 μM.

The index of performance has been computed by comparing the average values of salinity, water temperature, NO_3, NH_4, PO_4, DON and phytoplankton measured at the 14 stations of the bay in 2004 (Fig. 1), with their corresponding average modeled values (extracted for the corresponding sampling stations, at the corresponding sampling times). A large gradient between the ocean stations and the inner arms of the bay is observed in agreement with the observations (Camacho-Ibar et al., 2003).

Table 3 summarizes the statistics for each variable calculated on spatial variability over the observed data period (May-June 2004). As indicated by the R^2 values, more than 70 % of spatial variability of all variables (salinity, seawater temperature, NO_3, NH_4, PO_4, DON and phytoplankton) can be reproduced by the model, indicating that the model captures the general trends in these variables. The ME values indicate that the model performance was excellent to simulate salinity and water temperature (> 0.65), very good to simulate PO_4, NO_3, and NH_4, and good to simulate DON and phytoplankton. The model performance based on Pbias was excellent for salinity, water temperature, PO_4, and DON, very good for NH_4 and phytoplankton and good for NO_3.

The global model performance was explored by plotting R^2 vs RSD (R^2 and RSD should be close to one) of the values used to calculate the index of performance, confirming a good skill for all the variables with the exception of DON for which more accurate boundary data are required to adequately validate the model. In the eastern arm water exchange time is longer, dissolved inorganic nitrogen (DIN) supply from upwelled waters is very limited thus phytoplankton and *Ulva spp.* are little abundant and *Zostera marina* biomass is dominant. Thus, internal recycling in this area must be more intense. Then SQBFEEM requires an explicit module of seagrass which should increase DON concentrations to more “realistic” values.

Salinity and water temperature, followed by concentration of PO_4 and NO_3, show the best skill. Data limit did not allow us to further tune the model parameters to improve model calibration. The model slightly underestimates the variance of DON and NH_4 while overestimates the phytoplankton and NO_3 (Fig. 5). This is possibly related to the higher uncertainty and variability in the open boundary data of phytoplankton respect to the nutrients, which are less variable.

Model outputs of NO_3 have been compared with the available data collected at 14 stations (3–30; Fig. 1), sampled in spring (22, 26, 30 of May and 2, 5, 8 of June); and autumn (14, 17, 19, 22, 24, 28 of September and 1, 4, 11, 14 of October). The model was also able to reproduce the short-term variability, showing a good agreement with the measured values of NO_3 (as shown for the 3 stations 22, 26 and 19, located, respectively, close to the sea inlet (st. 22), in BFa (st. 26) and brazo SQ (st.19) (Fig. 6). The short-term evolution of spring and autumn is clearly influenced by upwelling conditions, that presented a stronger pulse in the first part of the spring (days between 22 of May and 12 of June), and less variable upwelling conditions during the autumn.

4.2. Response to upwelling variability

The response of N cycling, and of the primary and secondary producers to an increase and decrease in ocean-derived N loading induced by upwelling, was explored by comparing the results of the REF simulation with the LOW and HIGH scenarios.

In REF scenario, NO_3 is the dominant nutrient at the mouth of the lagoon in May-June (average concentration of 6.28 ± 0.68 μM) and September-October (average concentration of 1.36 ± 0.20 μM) (Fig. 4A), while NH_4 and DON are dominant, in particular during spring and summer, in the inner part of the lagoon (Fig. 4B, D). NH_4 concentrations are in average 2.70 ± 0.18 and 2.40 ± 0.23 μM in BFa and 2.09 ± 0.08 and 2.42 ± 0.23 μM in brazo SQ in May-June and September-October, respectively. The average of DON concentrations in May-June and September-October 2004 are, respectively, 8.0 ± 0.63 and 7.0 ± 0.45 μM in BFa and 9.40 ± 1.10 and 11.40 ± 0.50 μM in brazo SQ. McGlathery et al. (2007) indicate that it is common for DON content to be greater than the DIN content in semi-enclosed coastal ecosystems; and Berman and Bronk (2003) results also indicate that the observed DON concentrations of SQB (typically greater than 5 μM and often greater than 15 μM) (Rodriguez-Cardozo, 2004; unpublished results), are similar to those observed in this type of coastal systems.

Fig. 7 presents the time averaged values of NO_3 modeled results at the samplings stations (Fig. 1) for the three scenarios, during the spring upwelling conditions. NO_3 concentrations at the mouth of the bay (st. 3 to st. 8) are in agreement with the boundary inputs of, respectively, 3.6, 7.0 and 11.0 μM for REF, LOW and HIGH scenarios. NO_3 boundary concentration in HIGH scenario is three times that of LOW scenario, indicating that the supply of nutrients from the ocean to estuarine systems along the NE Pacific coast of America can have intense interannual variations (Camacho-Ibar et al., 2003; Ribas-Ribas et al., 2011). The spatial gradient of NO_3 highlights its ocean origins, as also confirmed by its inverse relationship with salinity (box in Fig. 7). In the HIGH scenario, NO_3 concentrations at the mouth of the bay were -in

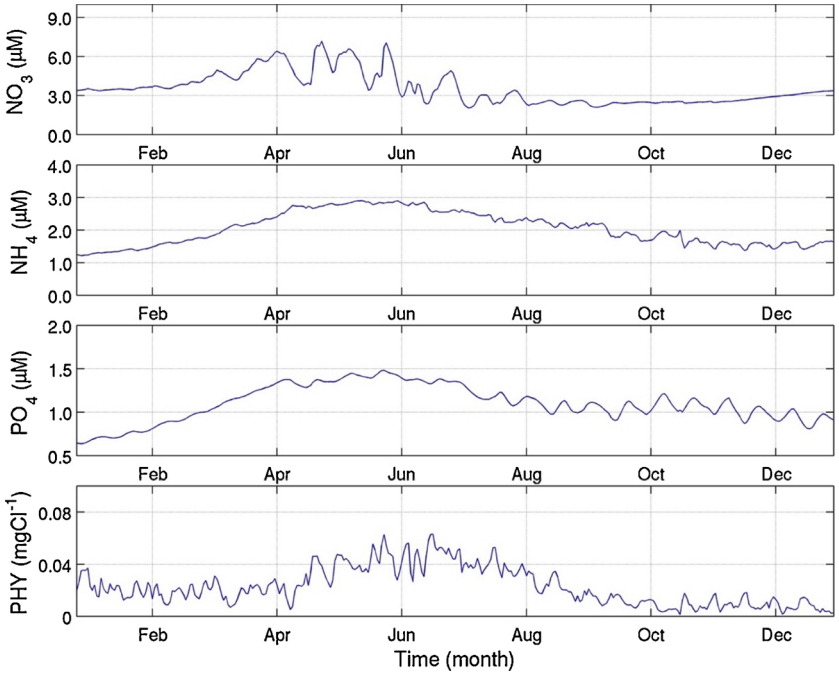

Fig. 3. Nutrients (NO_3, PO_4, NH_4) concentrations (µM) and phytoplankton biomass (mg C l^{-1}) time series for the entire simulation at the station 28 during 2004.

average- persistently above 10 µM (from st. 3–22) abruptly decreasing towards the inner end of brazo SQ. The LOW scenario, presents a lower NO_3 gradient from the mouth of the bay, with average concentration of NO_3 of 3.6 µM (Fig. 7), indicating that the NO_3 fluxes are minimum during weak upwelling. These results are also in agreement with previous analysis and measurements conducted during weak upwelling (Farfán and Álvarez-Borrego, 1983; Camacho-Ibar et al., 2003).

Maps in Fig. 8 show the spring average values of NO_3 (Fig. 8A) and phytoplankton (Fig. 8B) of REF scenario, and their corresponding anomalies in respect to LOW (Fig. 8C, D) and HIGH spring upwelling scenarios (Fig. 8E, F). Average values have been computed by averaging the model outputs between 1 April and 30 June 2004. The anomalies have been calculated at each point of the domain, as the difference between the values of the scenario (LOW or HIGH) in respect to the

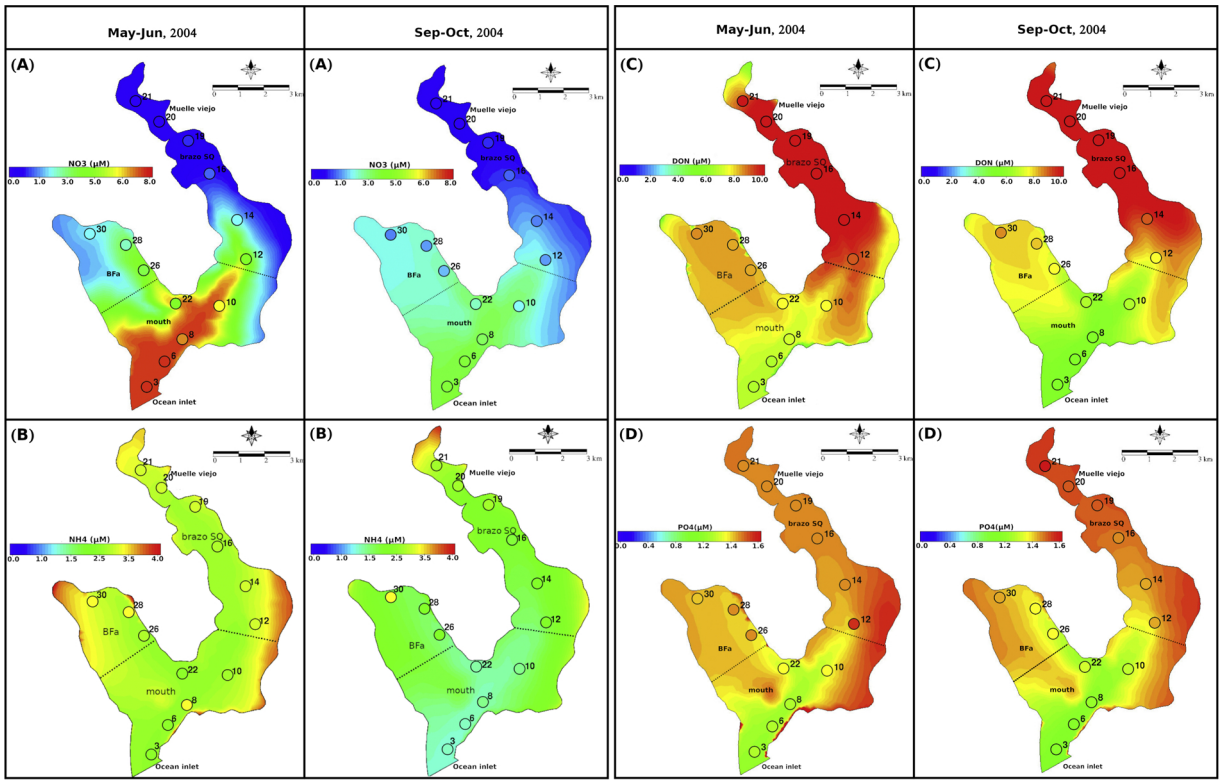

Fig. 4. Maps of simulated nutrients concentrations (in µM) of the REF scenario: (A) NO_3, (B) NH_4, (C) DON and (D) PO_4, compared with corresponding observations at the 14 sampling stations for May-June and September-October 2004.

Table 3
Results of the R^2 (variance), ME (Nash-Sutcliffe Efficiency) and Pbias (percentage model bias) for hydrological and biogeochemical variables, calculated for the model (3D-SHYFEM-SQBFEEM) of spring 2004. The index is categorized: dark grey = excellent, medium grey= very good and light grey= good.

Variable	R^2	ME	Pbias
NO_3	0.80	0.54	−21.36
NH_4	0.75	0.51	10.89
PO_4	0.82	0.64	8.99
DON	0.70	0.49	−2.65
Phytoplankton	0.74	0.27	−13.75
Salinity	0.94	0.80	0.71
Temperature	0.87	0.71	1.76

corresponding REF value.

The anomaly shown in Fig. 8E for the HIGH scenario highlights an increase in NO_3 concentration associated to the increasing upwelling intensity due to the stronger alongshore winds in the ocean adjacent to SQB registered during 2005 (Table 1). The anomaly is higher at the inlet, decreasing slightly toward the farther end of the BFa and brazo SQ, with values at the inlets up to ˜14 μM, 30 % higher than the maximum concentrations of ˜10 μM observed in REF scenario.

The opposite feature is observed in the LOW scenario, which presents a negative NO_3 anomaly of LOW scenario (Fig. 7C) throughout the lagoon with highest values at the inlet (associated to the decreased upwelling intensity) and lowest towards the brazo SQ.

Smith and Hollibaugh (1997) mention that the contributions of organic carbon from the adjacent ocean to Tomales Bay, California, control the seasonality of the net production of the ecosystem. The phytoplankton primary production due to upwelling in the CCS supplies labile organic carbon that is oxidized within the bay, which induces a net heterotrophic condition. Similar to Tomales Bay, SQB is also a net heterotrophic system where excess respiration is subsidized by the supply of particulate organic carbon from the adjacent sea (Camacho-Ibar et al., 2003).

The REF scenario simulation shows a decrease of phytoplankton from the mouth to brazo SQ (Fig. 8B), in agreement with Millan-Nuñez et al. (1982) observing for Chl-a, a decrease from 5 mg m^{-3} at the mouth to around 1 mg m^{-3} at the inner ends of the lagoon.

The phytoplankton anomaly of LOW scenario (Fig. 8D) is negative throughout the lagoon with highest values toward the brazo SQ and around the oyster farming area in BFa (Fig. 8B). Accordingly, in HIGH scenario (Fig. 8F) a positive phytoplankton anomaly throughout the lagoon is observed and gradually decreasing at the farther ends of brazo SQ. The positive phytoplankton anomaly in HIGH scenario (Fig. 8F) exhibits a correlated response to increased nutrient input in the mouth area (st. 3–22) in agreement with observations (Ribas-Ribas et al., 2011).

Predicted biomass of Ulva and oyster are sensitive to the upwelling scenarios. *Ulva spp*. and oyster biomass increase, respectively, about 35 % and 20 % under HIGH upwelling scenario, compared to the LOW one.

4.3. Nitrogen mass budget

A N mass budget was carried out by computing the N-fluxes and stocks of the SQBFEEM model variables (Fig. 2) under REF, LOW and HIGH upwelling scenarios for the spring period, during upwelling events. Sensitivity tests were made to explore how the model responds when using the same physical forcing of the REF scenario, but the boundary conditions of the HIGH scenario. The analysis showed that 35 % of the total variation of NO_3 stock was related to changes in physical forcing.

N-stocks and fluxes were computed by daily averaging the model outputs of NO_3, NH_4, DON, phytoplankton, zooplankton, *Ulva spp*., and oysters, and of their internal fluxes. The stock estimation was done by

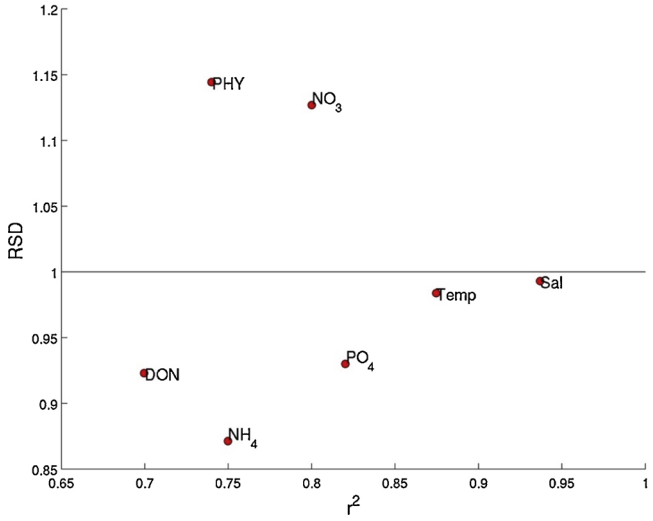

Fig. 5. Statistical parameters: a ratio of standard deviations (RSD) vs explained variance (r^2), obtained of the simulated nutrients (NO_3, PO_4, NH_4, DON) and phytoplankton (PHY), seawater temperature (Temp) and salinity (Sal), for May-June and September-October.

using stoichiometric relationships (Atkinson and Smith, 1983; Dame et al., 1989; Hecky et al., 1993) to convert the model variables into N units, while fluxes were obtained by computing and aggregating the source/sink terms of the model variables.

Fig. 9 shows the average values (over the spring period) of the N-stocks of the 8 aggregated variables and of their fluxes. N is imported into SQB from the ocean in different forms: N-NO_3, N-NH_4, N-DON, N-phytoplankton and N-zooplankton (Fig. 9). N-NO_3 is the biggest source of N, increasing with the increase in upwelling intensity. Total N-NO_3 loading from the ocean into the lagoon increased by a factor of ˜1.5 from LOW to HIGH and ˜1.2 from REF to HIGH scenario, ranging from ˜2.0–3.5 mmol N m^{-2} d^{-1} (Fig. 9). N-NO_3 contributes 65 and 80 %, respectively, of the total inputs of N in the LOW and HIGH scenarios. In the REF scenario, N-phytoplankton represents ˜10 % of the total imports of N; this value decreases when upwelling intensifies (6 % HIGH). The decrease in the contribution of phytoplankton import with upwelling intensification is due to the fact that phytoplankton biomass in the coastal upwelling waters is not only controlled by upwelling intensity, but by a combination of upwelling intensity and the duration of relaxation periods after upwelling events. According to Wilkerson et al. (2006), the ideal conditions for biomass accumulation are a combination of medium intensity upwelling and ˜4 to 5 days of relaxation. In other words, intense and persistent upwelling conditions such as those represented by our HIGH scenario may allow for high amounts of NO_3 to be advected, but physically damps the aggregation of phytoplankton cells.

The total fluxes of ocean N loading into the SQB (considering all sources, i.e. phytoplankton, zooplankton, DON, NO_3, NH_4) ranges from 3.50 to 4.40 mmol N m^{-2} d^{-1} in the LOW and HIGH scenarios, thus increasing by a factor of 1.30. Total N exports increase by a factor of 1.50, from 2.00–3.20 mmol N m^{-2} d^{-1} between LOW and HIGH scenarios, and thus the imbalance between imports and exports increases with upwelling intensification.

Moreover, advective N ocean loading exceeds the exports to the ocean and the lost through denitrification. As upwelling intensifies, N availability increases and a larger fraction of internal productivity is sustained by external inputs (Fig. 9).

The gross total imports of N-NO_3 into SQB estimated in this study are similar to the oceanic inputs into other estuarine systems influenced by upwelling along the California Current domain. Brown and Ozretich (2009) reported an average gross input of N-NO_3 into Yaquina Bay (Oregon, USA) of 3.3 × 10^5 mol d^{-1} during the dry season in the

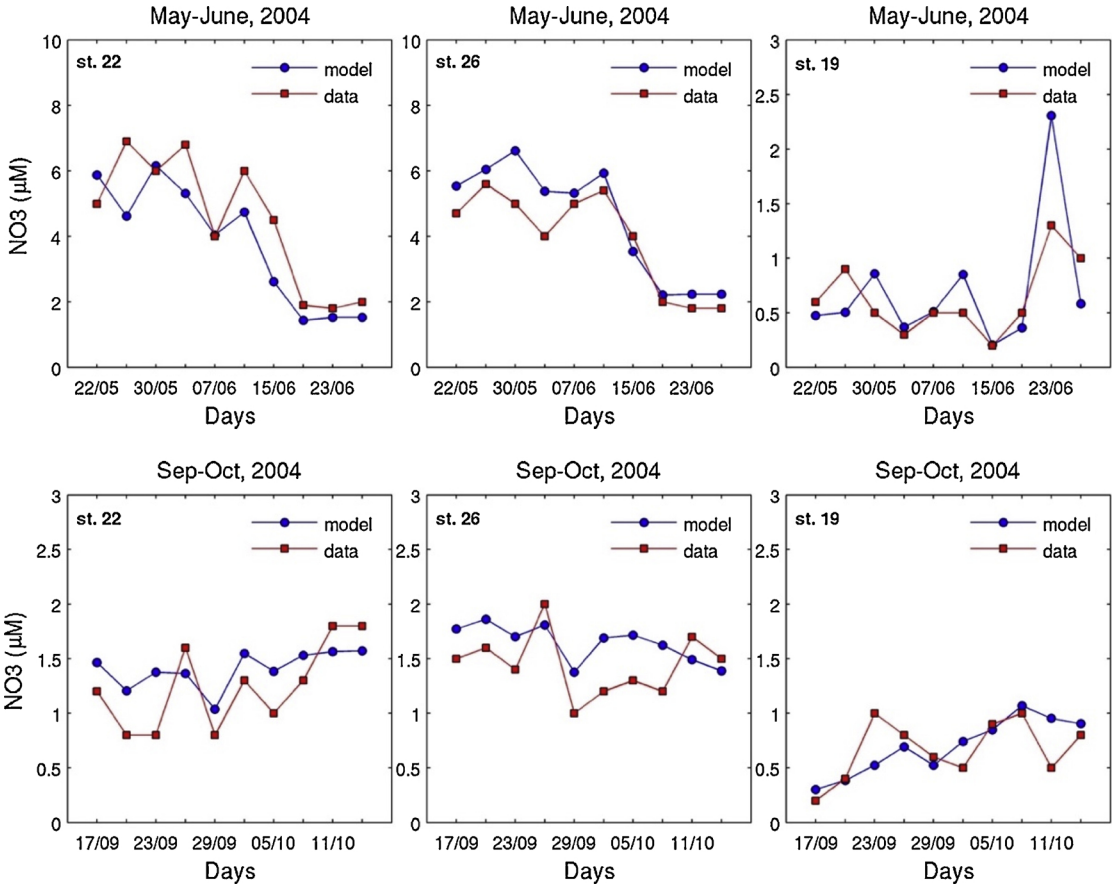

Fig. 6. Day-to-Day comparison of the simulated (blue circle) of the REF scenario and the observed (red square) NO_3 concentrations (in µM) during May-June and September-October 2004. (For interpretation of the references to colour in this figure legend, the reader is referred to the web version of this article).

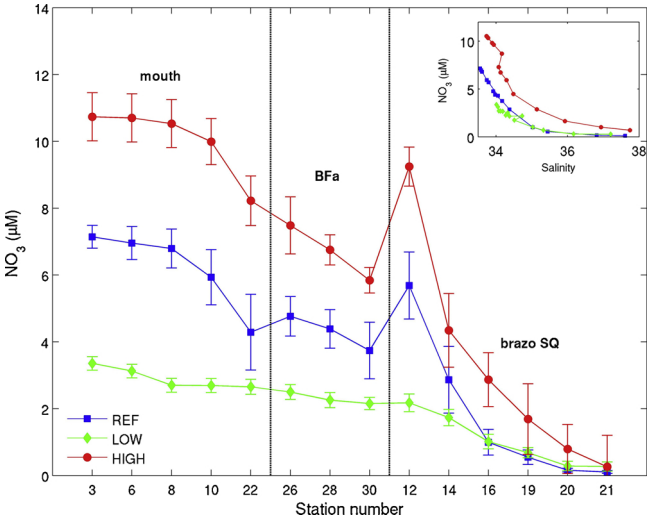

Fig. 7. Comparison of average NO_3 values (µM) predicted at the 14 sampling stations, ordered by the relative position from the Bay mouth, for the three scenarios, REF (blue square), LOW (green diamond) and HIGH (red circle). Upper-right corner: relationship between salinity vs. NO_3. (For interpretation of the references to colour in this figure legend, the reader is referred to the web version of this article).

1997–2003 period. An estimate of gross import of $NO_3 = 1.0 \times 10^5$ mol d^{-1} is obtained for Elkhorn Slough using the tidal prism volume (5.7×10^6 m^3) and the average N-NO_3 concentration in water during flooding tide (18 ± 8 µM) reported by Chapin et al. (2004). When gross imports are normalized to the corresponding surface area, even the highest rate of oceanic N-NO_3 supply into SQB (3.50 mmol m^{-2} d^{-1}) is 3 and 4 times lower than the loading into Elkhorn Slough (11 mmol m^{-2} d^{-1}) and Yaquina Bay (18 mmol m^{-2} d^{-1}) respectively.

Despite the absence of direct terrestrial loadings, loadings of N-NO_3 from the ocean to SQB are similar or even higher than loadings of N from land to some other shallow coastal lagoons subjected to low or moderate anthropogenic eutrophication. For example, other lagoons of similar size, such as Ria Formosa (Portugal; 58 km^2), Golfe de Fos (France; 42 km^2), and Bassin d'Arcachon (France; 155 km^2), receive N-NO_3 loadings of 0.50-1.50 mmol m^{-2} d^{-1} (Tett et al., 2003; de Wit et al., 2001), which is smaller than the oceanic N-NO_3 loading to SQB being double in the LOW scenario and 4 times higher during the HIGH scenario. This natural high loading of N from the ocean to SQB explains its high productivity, and is a good example of the strong control of upwelling on primary productivity of coastal lagoons and estuaries along the CCS, particularly during the dry season.

Despite the difference in gross loading, the net DIN loading estimated for the HIGH conditions in SQB (˜3.50 mmol m^{-2} d^{-1}) was similar to the average net loading of 4.0 mmol m^{-2} d^{-1} reported for Elkhorn Slough (Chapin et al., 2004), indicating that the retention of the oceanic DIN input in SQB is more efficient than the retention in Elkhorn Slough. N retention efficiency usually increases with residence time (Almroth-Rosell et al., 2016), therefore, the difference in retention efficiency is likely due to the fact that water residence time is larger in SQB because of its larger dimensions (the ratio of the surface areas being 4.6) as compared to Elkhorn Slough, with residence time of 5 days and surface area of 9.10 km^2 (Largier et al., 1997).

N-DON imports decrease with upwelling intensification since deep waters that are upwelled to the surface are depleted in DON (Letscher et al., 2013). Its contribution ranges between ˜17 % under LOW to ˜9

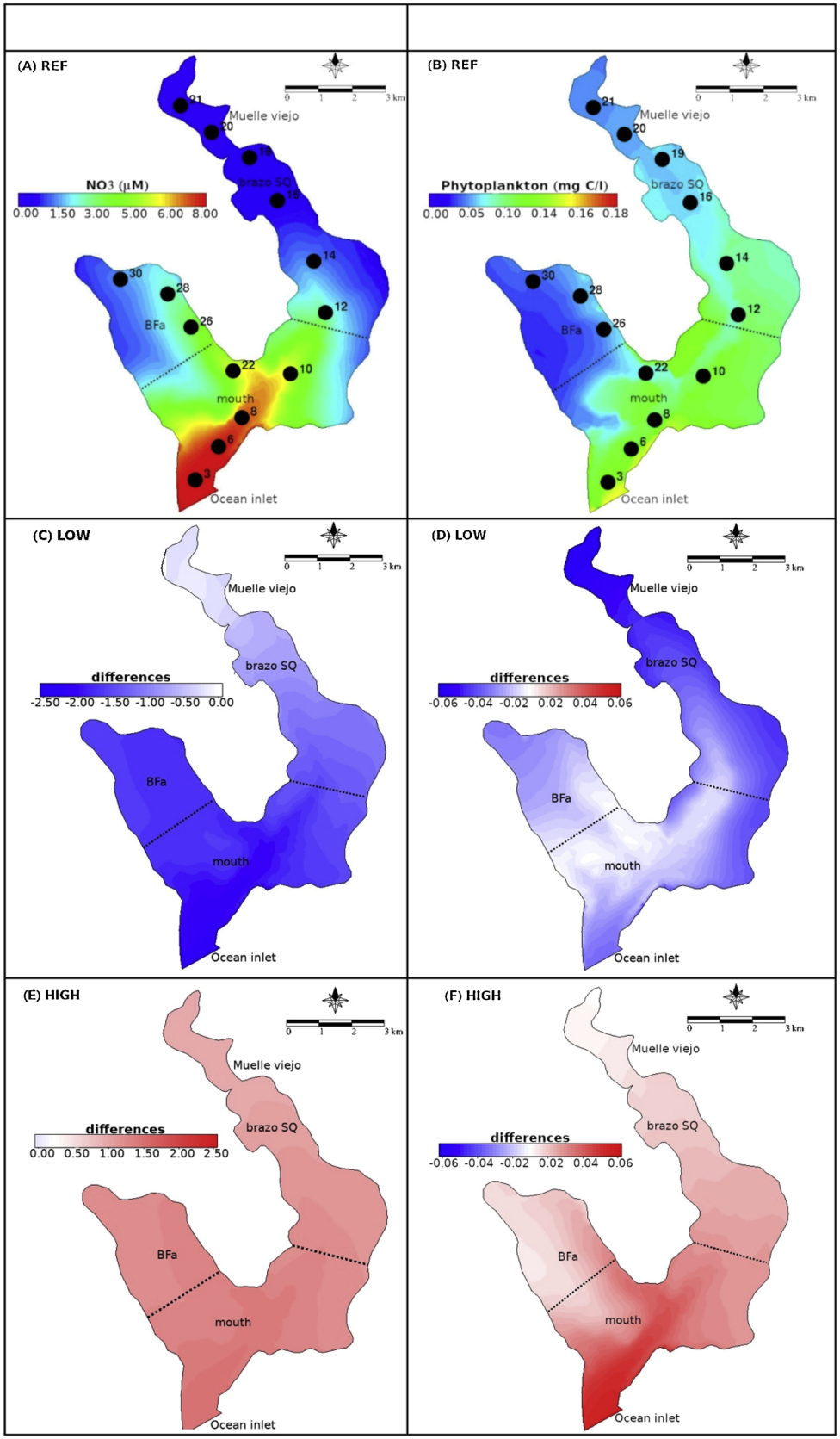

Fig. 8. (A) Spring average NO_3 concentration (µM) and (B) phytoplankton (mg C l^{-1}), predicted by the model SHYFEM-SQBFEEM, for the REF scenario, and corresponding anomalies calculated with LOW (C and D) and HIGH (E and F) scenarios.

and 10 %, respectively, under HIGH and REF scenarios (Fig. 9). During LOW scenario, upwelling strength is limited, and upwelled waters are enriched in DON inputs linked to the contribution of detritus rich waters produced locally (Letscher et al., 2013).

The western arm, BFa, is an area of oyster aquaculture (Fig. 1), where the activity of this bivalve likely plays a significant role on N cycling through phytoplankton ingestion, faeces and pseudofaeces (PON) production, and DIN (NH_4) excretion (Sandoval-Gil et al., 2016). In contrast, in brazo SQ where water exchange time is longer, DIN supply from upwelled waters is very limited and so phytoplankton are scarce. Internal recycling in BFa and brazo SQ is expected to be more intense. It is possible that the decomposing macroalgal mats (Fig. 1) contribute significant amounts of organic matter to the sediments (Ávila-López et al., 2017). Tyler et al. (2001) mentioned that in lagoonal systems with little riverine input the majority of new DON most likely comes from autochthonous macroalgae production or from enriched groundwater.

In the three scenarios of simulation more than 50–70 % of the primary production in the system is sustained by internal recycling of N (Fig. 9). This percentage was comparable to that found in other studies. For example, Flint et al. (1986) indicated that 90 % of the dissolved N supply for phytoplankton production is derived from sediments in the upper-estuary of Corpus Christi, whereas benthic regeneration supplies only 33 % of the dissolved N required for primary production outside the barrier island in coastal waters; Tyler et al. (2001) calculated that DON was an important component (52–98 %) of the total dissolved N pool in Hog Island Bay waters and made up the majority of the sediment N flux to the water column. In the case of SQB, residence time may be relatively low, therefore, the contribution of the N external supply tends to be higher compared to systems with higher residence times.

As expected, phytoplankton and *Ulva spp*. respond to N availability increasing their N uptake when N availability increases, during upwelling intensification (HIGH scenario). N uptake rates for phytoplankton ranges between 2.70–3.50 mmol N m^{-2} d^{-1} under LOW and HIGH scenario (Fig. 9), within the range found by Lara-Lara et al. (1980) of 8.0 and 76 mmol C m^{-2} d^{-1}, equivalent to variations of N incorporation rates between 1.20 and 12.0 mmol N m^{-2} d^{-1}.

Zooplankton N uptake rates through phytoplankton grazing was 1.30, 1.40 and 1.50 mmol N m^{-2} d^{-1} in the LOW, REF and HIGH scenarios, respectively (Fig. 9), in agreement with the values observed by Olivieri and Chavez (2000) of 1.30 mmol N m^{-2} d^{-1} at 5 m depth in Monterey Bay, California. Nevertheless, we do not have direct measurements of N-zooplankton dynamics in SQB, and our model was parameterized using values from the literature for other sites. The availability of direct measurements would provide results that are more robust. The ratio between N demand by N-phytoplankton and N-zooplankton was 2.2 and 2.3 under REF and HIGH, respectively, indicating that consumers are limited by primary productivity. The slight increase ratio with increasing upwelling suggests that consumers require more N than is supplied by primary productivity, thus partially relying on recycling to fulfill their N uptake demand.

N uptakes rates for Ulva ranges between 2.90 to 3.60 mmol m^{-2} d^{-1}. Observations show that under upwelling conditions, increasing DIN inputs favour the accumulation of *Ulva spp*. (Zertuche-González et al., 2009), that presents in SQB the common behaviour of opportunistic macroalgae (McGlathery et al., 2007; Viaroli et al., 2010). Camacho-Ibar et al. (2007) report values of 180 mmol N m^{-2} for *Ulva spp*. measured in spring-early summer 2004, during the upwelling season, when *Ulva spp.* biomass reaches its annual maximum (Aveytua-Alcázar et al., 2008). Our model confirms this response, showing stocks of N-*Ulva spp*. of 92 ± 9, 120 ± 18 and 140 ± 13 mmol N m^{-2} in LOW, REF and HIGH scenarios, respectively (Fig. 9), thus showing the influence of the oceanic nutrient inputs on its biomass confirming that *Ulva spp*. is a temporary N-sink, in agreement with observations by Zertuche-González et al. (2009).

The N-oysters stock shows a slight positive response to increasing N oceanic inputs in agreement with the results by Emery et al. (2016) who report no strong seasonal effects due to upwelling. In fact, the N-oysters stock increasing by a factor of 1.3 in HIGH scenario compared to LOW scenario (Fig. 9). The model reproduces the effect of oyster filtration activity showing a decreasing phytoplankton concentration in BFa compared to brazo SQ (Fig. 8B) (and compared to the simulation performed without the oyster farm, not shown). Recently a study of resource use of cultured oysters in SQB indicated that phytoplankton were most important as a food source at the oceanic site and its role decreased up the lagoon where Ulva represented up to 50 % of their diet (Emery et al., 2016).

The total N-phytoplankton demand by oysters was 0.70, 0.80 and 1.0 mmol N m^{-2} d^{-1} under LOW, REF and HIGH, respectively (Fig. 9). These rates are of the same order in other sites (1.0–5.0 mmol N m^{-2} d^{-1}) as those reported by Dumbauld et al. (2009). Removing oyster farms, N accumulates in N-phytoplankton and N-zooplankton.

In our model, the total N loading is balanced by exportation, denitrification and biomass accumulation in primary producers. Denitrification accounts for a significant fraction of the N imbalance; ~43 % under LOW and REF and 46 % under HIGH. Denitrification rates increase (1.5–2.0 mmol N m^{-2} d^{-1}, under LOW and HIGH, respectively) as N-loading increases (Fig. 9). So, the sediments play an important role in the total N-losses from the system.

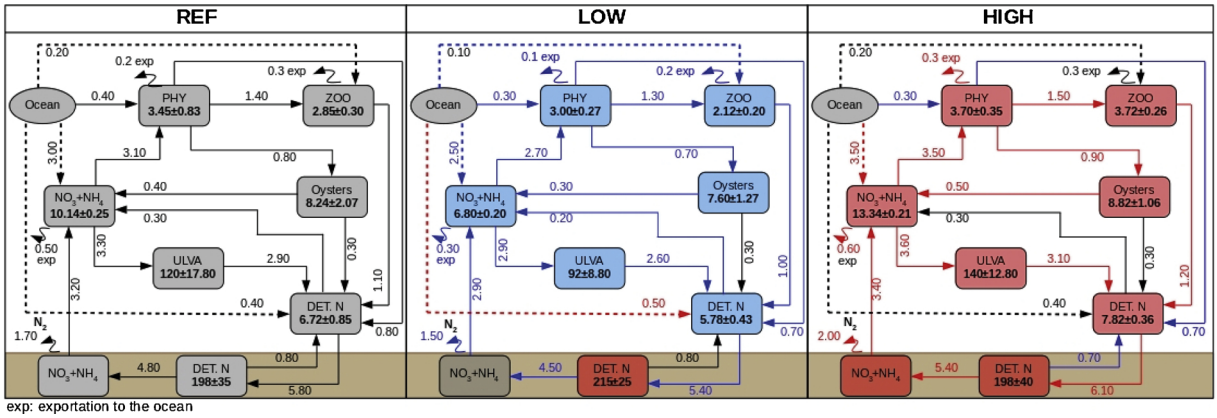

Fig. 9. Computed N spring budget (stocks and fluxes) in SQB over the three upwelling scenarios. Note that the blue and red colours refer to negative and positive variation of the stocks and fluxes in respect to the REF scenario. Stocks in mmol N m^{-2} and fluxes in mmol N m^{-2} d-. (For interpretation of the references to colour in this figure legend, the reader is referred to the web version of this article).

5. Conclusions

In this work, an ecological model simulating the 3-D hydrodynamics and biogeochemistry was implemented in SQB, a coastal lagoon located in the CCS. The model reproduces the spatial and temporal evolution of nutrient, phytoplankton, zooplankton, oysters and *Ulva spp*. An N budget is calculated under different upwelling conditions, also analysing how the variation in the oceanic exchanges -and in particular changes in upwelling intensity and frequency, also related to an scenario of climate change- alters the biogeochemical processes of the SQB. Comparison with available data and observations, confirm the model capability to reproduce the main features and variability within daily, seasonal and interannual scales of both physical (excellent capabilities) and biogeochemical (very good capabilities) processes.

The model shows that upwelling intensity has a large influence on N availability and consumption within the bay, and the response of primary and secondary producers. The contribution of upwelling is of particular importance for systems like SQB which have limited inputs of nutrient of terrigenous origin, and mainly rely on the oceanic inputs of organic matter and nutrients. Upwelled waters, rich in phytoplankton and nutrients, particularly NO_3, stimulate the autochthonous production, which is limited by N availability. In fact, the differences between average value of major parameters observed in HIGH and LOW upwelling conditions of about 25 % for phytoplankton, 20 % for oyster and more than 40 % for zooplankton.

This result can be used to set a range of expected variability in oyster production related to the expected variability in upwelling regimes, thus contributing to a science based management of this important socio-economic activity. This can in turn be used to support the valuation of the ecosystem services related to the range of upwelling variability, by relating the impacts of changes in upwelling regimes and N inputs to the local productivity in SQB and on the economic activities relying on it.

Acknowledgments

This work was funded by research grant provided by “Ministero degli Affari Esteri” under the program of scientific and technological collaboration between Italy and Mexico and through the SEP-CONACYT (Mexico) project “Integral study of the Nitrogen cycling in Bahia Falsa, Baja California” (ref. no. CONACYT-UABC CB-2010-01-154376) awarded to V.F.C.I. We thank the members of the Geosciences group of the “Instituto de Investigaciones Oceanológicas (IIO)” who performed the measurements and kindly provided the dataset. We thank Georg Umgiesser for provided helpful technical advice and support to SHYFEM model. We thank Valentina Mosetti for contributed with the editing of map of San Quintin Bay.

Appendix A

Table A2

Table A1
Symbols and values of model (SQBFEEM) parameters.

	Symbol	Unit	Value	Reference
Phytoplankton				
Death rate constant	K1D	d^{-1}	0.120	Umgiesser et al. (2003)
Growth rate constant	K1C	d^{-1}	1.650	Umgiesser et al. (2003)
Growth rate	K1T	°C	1.068	Umgiesser et al. (2003)
Nitrogen half saturation constant for growth	KMNG1	mg N l^{-1}	0.090	Estimated in this work
Phosphorus half saturation constant for growth	KMPG1	mg P l^{-1}	0.014	Estimated in this work
Respiration rate constant	K1RC	d^{-1}	0.096	Umgiesser et al. (2003)
Respiration rate temperature constant	K1RT	————	1.068	Umgiesser et al (2003)
Optimal value of light intensity for growth	IS2	W m^{-2}	200.0	Umgiesser et al (2003)
Nitrogen/Carbon ratio	NC	mg N mg C^{-1}	0.115	Estimated in this work
Phosphorus/Carbon ratio	PC	mg P mg C^{-1}	0.025	Estimated in this work
Oxygen /Carbon ratio	OC	mg O_2 mg C^{-1}	2.660	Estimated in this work
Zooplankton				
Death rate constant	KDZ	d^{-1}	0.150	Umgiesser et al. (2003)
Grazing efficiency	EFF	———	0.500	Umgiesser et al. (2003)
Grazing rate constant	KGRZ	d^{-1}	1.200	Umgiesser et al. (2003)
Half sat. constant for phytoplankton in grazing	KPHYZ	———	0.500	Umgiesser et al. (2003)
Ulva spp.				
Death rate coefficient	KMTU1	h^{-1}	0.840	Aveytua Alcázar et al. (2008)
Death rate coefficient	KMTU2	h^{-1}	0.002	Aveytua Alcázar et al. (2008)
Death rate maxima	PKMTDO	h^{-1}	1.000	Solidoro et al. (1997)
Growth rate constant	PVGUD	d^{-1}	0.450	Solidoro et al. (1997)
Respiration rate constant	PVRU	mg O_2 g dw h^{-1}	2.500	Solidoro et al. (1997)
Uptake rate of nitrate	PVNOU	mg N g dw h^{-1}	0.900	Aveytua Alcázar et al. (2008)
Uptake rate of ammonium	PVNHU	mg N g dw h^{-1}	3.200	Aveytua Alcázar et al. (2008)
NH4 half saturation constant for growth	PKNHU	mg N l^{-1}	0.600	Solidoro et al. (1997)
NO3 half saturation constant for growth	PKNOU	mg N l^{-1}	0.060	Solidoro et al. (1997)
PO4 half saturation constant for Ulva	PKPO4	mg PO_4 l^{-1}	0.01	Solidoro et al. (1997)
Maximum quota	PQMAX	mg N g dw^{-1}	45.00	Solidoro et al. (1997)
Minimum quota	PQMIN	mg N g dw^{-1}	10.00	Solidoro et al. (1997)
Critical nitrogen quota level	PQLC	mg N g dw^{-1}	8.000	Solidoro et al. (1997)
Temperature coefficient for growth	PUGT1	$°C^{-1}$	0.200	Solidoro et al. (1997)
Temperature coefficient for growth	PUGT2	°C	12.50	Solidoro et al. (1997)
Temperature coefficient for respiration	PURT1	$°C^{-1}$	0.300	Solidoro et al. (1997)
Temperature coefficient for respiration	PURT2	°C	10.00	Solidoro et al. (1997)
Maximum oxygen production	PPMAX	mg O_2 g dw h^{-1}	20.00	Solidoro et al. (1997)
Coefficient for light	PUGL1	———	8.67	Solidoro et al. (1997)

(*continued on next page*)

Table A1 (*continued*)

	Symbol	Unit	Value	Reference
Conversion factor	PKPAR	——	0.46	Solidoro et al. (1997)
Light extinction coefficient	PKEST	——	1.00	Aveytua Alcázar et al. (2008)
Crassostrea gigas				
Maximal filtration rate	KFILT	d^{-1}	0.020	García-Esquivel et al. (2004)
Filtration efficacy coefficient	EFFSHELL	———	2.500	Chapelle et al. (2000)
Semisaturation const. for phytoplankton filtration	KPHY	———	0.800	Chapelle et al. (2000)
Decay rate constant	KDEC	d^{-1}	0.001	García-Esquivel et al. (2004)
Semisaturation const. for shellfish growth	KSHELL	———	0.800	Chapelle et al. (2000)
% Biodeposition	BDSHELL	%	0.300	Chapelle et al. (2000)
Sediment				
Fraction of nutrient sink	KWSINK	$m\ d^{-1}$	3.00	Estimated in this work
Organic phosphorous temp. coefficient	KPT	———	1.00	Estimated in this work
Water velocity semisaturation	Kvel	——	0.02	Estimated in this work
Fraction of particulate organic phosphorus	FRACPOP	———	0.50	Estimated in this work
Fraction of particulate organic nitrogen	FRACPON	———	0.01	Estimated in this work
Fraction of phosphorus resuspended	KPRESUSP	$m\ d^{-1}$	0.10	Estimated in this work
Fraction of nitrogen resuspended	KNRESUSP	$m\ d^{-1}$	0.10	Estimated in this work
Half saturation constant for phosphorus	KPCSED	———	0.01	Estimated in this work
Half saturation constant for nitrogen	KNCSED	———	0.10	Estimated in this work
Mineralisation temperature coefficient	KNT	——	1.08	Estimated in this work

Table A2
Macroalgae, Oyster and sediment functional expressions of the SQBFEEM.

Ulva spp.	
$GUSP = PVGUD * \left(\frac{Quota - PQMIN}{Quota - PQLC}\right) * FUGL * FUGT * FUPL$	1.Growth function with nutrient, temperature and light limitation.; where Quota is a intratissual nitrogen
$FUGL = 1 - exp\left(\frac{Fi0}{PUGL1}\right)$	2.Light limitation function
$Fi0 = qrad * PKPAR * exp(-PKEST * depth)$	3.Light limitation function
$FUGT = \left(\frac{1}{1 + exp(-PUGT1 * (stp - PUGT2))}\right)$	4.Temperature limitation function for growth
$FURT = \left(\frac{1}{1 + exp(-PURT1 * (stp - PURT2))}\right)$	5.Temperature limitation function for respiration
$FUPL = PO4\left(\frac{PKPO4}{PO4}\right)$	6. Phosphate limitation function
$MTU = min(KMTU2 * (U ** KMTU1), PKMTDO * U)$	7.Mortality function; where U is biomass
$RU = (PVRU * FURT * U)$	8.Respiration function
$FU = \left(\frac{PPMAX}{PVGUD}\right) * GUSP * U$	9. Photosynthesis function
$TSNH4 = \left(\frac{PVNHU * NH4}{NH4 + PKNHU}\right) * \left(\frac{PQMAX - QUOTA}{PQMAX - PQMIN}\right)$	10.Ammonium uptake
$TSNO3 = \left(\frac{PVNOU * NO3}{NOX + PKNOU}\right) * \left(\frac{PQMAX - QUOTA}{PQMAX - PQMIN}\right)$	11.Nitrate uptake
Crassostrea gigas	
$FILT = KFILT * SHELLFARM * SHELLSIZE * VOL * \left(\frac{PHYT}{KPHY + PHY}\right)$	12.Filtration function; where VOL is volumen
$SHELLG = FILT * \left(\frac{EFFSHELL}{KSHELL + SHELLSIZE}\right)$	13.Growth function
$MORSHELL = (SHELLFARM * KDEC * VOL)$	14.Mortality function
Sediment	
$Q(NH4)sed = (VOLsed * KNCSED * KNT ** (t - 20) * ONsed)$	15.Mineralisation of ON in sediment
$Q(ON)sed = (VOLsed * KNRESUSP * fvel * ONsed - ONsink)$	16.Resuspension of ON from sediment
$ONsink = vol * \left(1 - exp\frac{-dt}{taun}\right) * ON * \left(\frac{FRACPON}{dt}\right)$	17.Sink of ON from the water column
$Q(OPO4)sed = (VOLsed * KPCSED * KPT ** (t - 20) * OPsed)$	18.Mineralization of OP in sediment
$Q(OP)sed = (VOLsed * KPRESUSP * fvel * OPsed - OPsink)$	19.Resuspension of OP from sediment
$OPsink = vol * \left(1 - exp\frac{-dt}{taup}\right) * OP * \left(\frac{FRACPOP}{dt}\right)$	20.Sink of OP from the water column
$fvel = \frac{(vel * vel)}{(vel + kvel)}$	21.Velocity functional expression for sinking and resuspension
$taup{=}taun = \frac{(depth)}{(WSINK)}$	22.Sinking parameter
$WSINK = kWSINK * (1 - fvel)$	23.Sinking velocity

References

Aguirre-Muñoz, A., Buddemeir, R.W., Camacho-Ibar, V.F., Carriquiry, J.D., Ibarra-Obando, S.E., Massey, W.B., Smith, S.V., Wulff, F., 2001. Sustainability of coastal resources in San Quintin, Mexico. Ambio 30, 142–149.

Allen, J.I., Somerfield, P.J., Gilbert, F.J., 2007. Quantifying uncertainty in high-resolution coupled hydrodynamic-ecosystem models. J. Mar. Syst. 64, 3–14.

Almroth-Rosell, E., Edman, M., Eilola, K., Markus-Meier, H.E., Sahlberg, J., 2016. Modelling nutrient retention in the coastal zone of a eutrophic sea. Biogeosciences 13, 5753–5769.

Arellano, B., Rivas, D., 2019. Coastal upwelling will intensify along the Baja California

coast under climate change by mid-21st century: insights from a GCM-nested physical-NPZD coupled numerical ocean model. J. Mar. Syst. 199, 103207.
Atkinson, M.J., Smith, S.V., 1983. C:N:P ratios of benthic marine plants. Limnol. Oceanogr. 28, 568–574.
Aveytua-Alcázar, L., Camacho-Ibar, V.F., Souza, A.J., Allen, J.I., Torres, R., 2008. Modelling *Zostera marina* and *Ulva spp*. in a coastal lagoon. Ecol. Modell. 218, 354–366.
Ávila-López, M.C., Hernández-Ayón, J.M., Camacho-Ibar, V.F., Sandoval-Gil, J.M., Mejía-Trejo, A., Pacheco-Ruiz, I., 2017. Air-water CO2 fluxes and net ecosystem production changes in a Baja California Coastal Lagoon during the anomalous North Pacific warm condition. Estuaries Coasts 40, 792–806.
Bakun, A., Black, B.A., Bograd, S.J., García-Reyes, M., Miller, A.J., Rykaczewski, R.R., Sydeman, W.J., 2015. Anticipated effects of climate change on coastal upwelling ecosystems. Curr. Clim. Change Rep. 1, 85–93.
Banas, N.S., Hichey, B.M., Newton, J.A., Ruesink, J.L., 2007. Tidal exchange, bivalve grazing, and patterns of primary production in Willapa Bay, Washington, USA. Mar. Ecol. Prog. Ser. 341, 123–139.
Berman, T., Bronk, D.A., 2003. Dissolved organic nitrogen: a dynamic participant in aquatic ecosystems. Aquat. Microb. Ecol. 31, 279–305.
Brown, C.A., Ozretich, R.J., 2009. Coupling between the coastal ocean and Yaquina Bay, Oregon: importance of oceanic inputs relative to other nitrogen sources. Estuaries Coasts 32, 219–237.
Camacho-Ibar, V.F., Carriquiry, J.D., Smith, S.V., 2003. Non-conservative P and N fluxes and net ecosystem production in San Quintín Bay, México. Estuaries 26 (5), 1220–1237.
Camacho-Ibar, V.F., Hernández-Ayón, J.M., Santamaría-del-Angel, E., Daesslé-Heuser, L.W., Zertuche-González, J.A., 2007. In: Hernández-de laTorre, B., Gaxiola-Castro, G. (Eds.), Relación de las surgencias con los stocks de carbono en Bahía San Quintín, una laguna costera del NW de México. Carbono en Ecosistemas Acuáticos de México. INE, CICESE, pp. 355–370.
Chapelle, A., Ménesguen, A., Deslous-Paoli, J.M., Souchu, P., Mazouni, N., Vaquer, A., Millet, B., 2000. Modelling nitrogen, primary production and oxygen in a Mediterranean lagoon. Impact of oysters farming and inputs from the watershed. Ecol. Modell. 127, 161–181.
Chapin, T.P., Caffrey, J.M., Jannasch, H.W., Coletti, L.J., Haskins, J.C., Johnson, K.S., 2004. Nitrate sources and sinks in Elkhorn Slough, California: results from long-term continuous *in situ* nitrate analyzers. Estuaries 27, 882–894.
Chavez, F.P., 2012. Climate change and marine ecosystems. PNAS 109 (47), 19045–19046.
Chenillat, F., Riviere, P., Capet, X., Franks, P.J., Blanke, B., 2013. California Coastal Upwelling Onset Variability: cross-shore and bottom-up propagation in the planktonic ecosystem. PLoS One 8 (5), e62281. https://doi.org/10.1371/journal.pone.0062281.
Colbert, D., McManus, J., 2003. Nutrient biogeochemistry in an upwelling-influenced estuary of the Pacific northwest (Tillamook Bay, Oregon, USA). Estuaries 26, 1205–1219.
Dame, F.R., Spurrier, J.D., Wolaver, T.G., 1989. Carbon, nitrogen and phosphorus processing by an oyster reef. Mar. Ecol. Prog. Ser. 54, 249–256.
de Wit, R., et al., 2001. ROBUST: the role of buffering capacities in stabilizing coastal lagoon ecosystems. Cont. Shelf Res. 21, 2021–2041.
Dumbauld, B.R., Ruesink, J.L., Rumrill, S.S., 2009. The ecological role of bivalve shellfish aquaculture in the estuarine environment: a review with application to oyster and clam culture in West Coast (USA) estuaries. Aquaculture 290, 196–223.
Emery, K.A., Wilkinson, G.M., Camacho-Ibar, V.F., Pace, M.L., McGlathery, K.J., Sandoval-Gil, J.M., Hernández-López, J., 2016. Resource use of an aquacultured oyster (Crassostrea gigas) in the reverse estuary Bahia San Quintín, Baja California, México. Estuaries Coasts 39, 866–874.
Farfán, B.C., Álvarez-Borrego, S., 1983. Variability and fluxes of nitrogen and organic carbon at the mouth of a coastal lagoon. Estuar. Coast. Shelf Sci. 17, 599–612.
Fiechter, J., Edwards, C.A., Moore, A.M., 2018. Wind, Circulation, and Topographic effects on alongshore phytoplankton variability in the California current. Geophys. Res. Lett. 45, 3238–3245. https://doi.org/10.1002/2017GL076839.
Flint, R.W., Powell, G.L., Kalke, R.D., 1986. Ecological effects from the balance between new and recycled nitrogen in Texas coastal waters. Estuaries 9, 284–294.
García-Esquivel, Z., González-Gomez, M.A., Ley-Lou, F., Mejia-Trejo, A., 2004. Oyster culture in the west arm of San Quintin Bay: current biomass and preliminary estimate of the carrying capacity. Cienc. Mar. 30 (1A), 61–74.
García-Reyes, M., Sydeman, W.J., Scoeman, D.S., Rykaczewski, R.R., Black, B.A., Smith, A.J., Bograd, S.J., 2015. Under pressure: climate change, upwelling, and eastern boundary upwelling ecosystems. Front. Mar. Sci. https://doi.org/10.3389/fmars.2015.00109.
Gracia-Escobar, M.F., Millán-Núñez, R., González-Silvera, A., Santamaría-del-Ángel, E., Camacho-Ibar, V.F., Trees, C.C., 2014. Changes in the abundance and composition of phytoplankton in a coastal lagoon during neap-spring tide conditions. Open J. Mar. Sci. 4, 80–100.
Hecky, R.E., Campbell, P., Hendzel, L.L., 1993. The stoichiometry of carbon, nitrogen, and phosphorus in particulate matter of lakes and oceans. Limnol. Oceanogr. 38 (4), 709–724.
Hickey, B.M., Banas, N.S., 2003. Oceanography of the U.S. Pacific Northwest coast and estuaries with application to coastal ecology. Estuaries 26 (4B), 1010–1031.
Ibarra-Obando, S., Camacho-Ibar, V.F., Carriquiry, J.D., Smith, S.V., 2001. Upwelling and lagoonal ecosystems of the dry Pacific coast of Baja California. In: Seeliger, U., Kjerfve, B. (Eds.), Coastal Marine Ecosystems of Latin America. Springer-Verlag, Germany, pp. 315–329.
Ibarra-Obando, S.E., Smith, S.V., Poumian-Tapia, M., Camacho-Ibar, V.F., Carriquiry, J.D., Montes-Hugo, M., 2004. Benthic metabolism in San Quintin Bay, Baja California, Mexico. Mar. Ecol. Prog. Ser. 283, 99–112.
Lara-Lara, J.R., Álvarez-Borrego, S., Small, L.F., 1980. Variability and tidal exchange of ecological properties in a coastal lagoon. J. Estuaries Coast. Mar. Sci. 11, 613–637.
Largier, J.L., Hollibaugh, J.T., Smith, S.V., 1997. Seasonally hypersaline estuaries in Mediterranean-climate regions. Estuar. Coast. Shelf Sci. 45, 789–797.
Letscher, R.T., Hansell, D.A., Carlson, C.A., Lumpkin, R., Knapp, A.N., 2013. Dissolved organic nitrogen in the global surface ocean: distribution and fate. Global Biogeochem. Cycles 27, 141–153.
McGlathery, K.J., Sundbäck, K., Anderson, I.C., 2007. Eutrophication in shallow coastal bays and lagoons: the role of plants in the coastal filter. Mar. Ecol. Prog. Ser. 348, 1–18.
Melaku Canu, D., Umgiesser, G., Solidoro, C., 2001. Short-term simulations under winter conditions in the lagoon of Venice: a contribution to the environmental impact assessment of temporary closure of the inlets. Ecol. Modell. 138 (1–3), 215–230.
Melaku Canu, D., Solidoro, C., Umgiesser, G., 2003. Modelling the responses of the Lagoon of Venice ecosystem to variations in physical forcings. Ecol. Modell. 170, 265–289.
Melaku Canu, D., Campostrini, P., Dalla Riva, S., Pastres, R., Pizzo, L., Rossetto, L., Solidoro, C., 2011. Addressing sustainability of clam farming in the Venice Lagoon. Ecol. Soc. 16 (3), 26. https://doi.org/10.5751/ES-04263-160326.
Melaku Canu, D., Solidoro, C., Umgiesser, G., Cucco, A., Ferrarin, C., 2012. Assessing confinement in coastal lagoons. Mar. Pollut. Bull. 64 (11), 2391–2398.
Melaku Canu, D., Aveytua-Alcázar, L., Camacho-Ibar, V.F., Querin, S., Solidoro, C., 2016. Hydrodynamic properties of San Quintin Bay, Baja California: merging models and observations. Mar. Pollut. Bull. 108 (1–2), 203–214.
Millan-Nuñez, R., Álvarez-Borrego, S., Nelson, D.M., 1982. Effects of physical phenomena on the distribution of nutrients and phytoplankton productivity in a coastal lagoon. Estuar. Coast. Shelf Sci. 15, 317–335.
Olivieri, R.A., Chavez, F.P., 2000. A model of plankton dynamics for the coastal upwelling system of Monterrey Bay, California. Deep-Sea Res. II 47, 1077–1106.
Parsons, T.R., Takahash, I.M., Hargrave, B., 1984. Biological Oceanographic Processes. Pergamon, Oxford, pp. 330.
Pastres, R., Solidoro, C., Cossarini, G., Melaku Canu, D., Dejak, C., 2001. Managing the rearing of Tapes philippinarum in the lagoon of Venice: a decision support system. Ecol. Modell. 138 (1–3), 231–245.
Pennington, T.J., Chavez, F.P., 2000. Seasonal fluctuations of temperature, salinity, nitrate, chlorophyll and primary production at station H3/M1 over 1989-1996 in Monterey Bay, California. Deep-Sea Res. II 47, 947–973.
Ribas-Ribas, M., Hernández-Ayon, J.M., Camacho-Ibar, V.F., Cabello-Pasini, A., Mejia-Trejo, A., Durazo, R., Galindo-Bect, S., Souza, A.J., Forja, J.M., Siqueiros-Valencia, A., 2011. Effects of upwelling, tides and biological processes on the inorganic carbon system of a coastal lagoon in Baja California. Estuar. Coast. Shelf Sci. 95 (45), 367–376.
Rodriguez-Cardozo, L., 2004. Evaluación del nitrógeno orgánico disuelto en los balances de nitrógeno en Bahía San Quintín, B.C. Bachelor Thesis. Universidad Autonoma de Baja California, Facultad de Ciencias Marinas.
Ruesink, J., Roegner, C., Dumbauld, B., Newton, J., Armstrong, D., 2003. Contributions of coastal and watershed energy sources to secondary production in a Northeastern Pacific estuary. Estuaries 26, 1079–1093.
Sandoval-Gil, J.M., Alexandre, A., Santos, R., Camacho-Ibar, V.F., 2016. Nitrogen uptake and internal recycling in *Zostera marina* exposed to oyster farming: eelgrass potential as a natural biofilter. Estuaries Coasts 39 (6), 1694–1708.
Smith, S.V., Hollibaugh, J.T., 1997. Annual cycle and interannual variability of ecosystem metabolism in a temperate climate embayment. Ecol. Monogr. 67, 509–533.
Solidoro, C., Pecenik, G., Pastres, R., Franco, D., Dejak, C., 1997. Modelling macroalgae (*Ulva rigida*) in the Venice lagoon: Model structure identification and first parameters estimation. Ecol. Modell. 94, 191–206.
Solidoro, C., Pastres, R., Melaku Canu, D., Pellizzato, M., Rossi, R., 2000. Modelling the growth of *Tapes philippinarum* in Northern Adriatic lagoons. Mar. Ecol. Prog. Ser. 199, 137–148. https://doi.org/10.3354/meps199137.
Solidoro, C., Melaku Canu, D., Cucco, A., Umgiesser, G., 2004. A partition of the Venice Lagoon based on physical properties and analysis of general circulation. J. Mar. Syst. 51 (1–4), 147–160.
Tett, P., Gilpin, L., Svendsen, H., Erlandsson, C.P., Larsson, U., Kratzer, S., Janzen, C., Lee, J.Y., Grenz, C., Newton, A., Ferreira, J.G., Fernandes, T., Scoty, S., 2003. Eutrophication and some European waters of restricted exchange. Cont. Shelf Res. 23, 1635–1671.
Tyler, A.C., McGlathery, K.J., Anderson, I.C., 2001. Macroalgae mediation of dissolved organic nitrogen fluxes in a temperate coastal lagoon. Estuar. Coast. Shelf Sci. 53, 155–168.
Umgiesser, G., Melaku Canu, D., Solidoro, C., Ambrose, R., 2003. A finite element ecological model: a first application to the Venice Lagoon. Environ. Model. Softw. 18, 131–145.
Umgiesser, G., Melaku Canu, D., Cucco, A., Solidoro, C., 2004. A finite element model for the Venice Lagoon. Development, set up, calibration and validation. J. Mar. Syst. 51 (1), 123–145.
Umgiesser, G., Ferrarin, C., Cucco, A., De Pascalis, F., Bellafiore, D., Ghezzo, M., Bajo, M., 2014. Comparative hydrodynamics of 10 Mediterranean lagoons by means of

numerical modeling. J. Geophys. Res. Oceans 119, 2212–2226. https://doi.org/10.1002/2013JC009512.

Viaroli, P., Azzoni, R., Bartoli, M., Giordani, G., Naldi, M., Nizzoli, D., 2010. Primary productivity, biogeochemical buffers and factors controlling trophic status and ecosystem processes in Mediterranean coastal lagoons: a synthesis. Adv. Oceanogr. Limnol. 1 (2), 271–293. https://doi.org/10.1080/19475721.2010.528937.

Ward, D.H., Morton, A., Tibbitts, T.L., Douglas, D.C., Carrera-González, E., 2003. Long-term in eelgrass distribution at Bahia san Quintin, Baja California, México, using satellite imagery. Estuaries 26 (6), 1529–1539.

Xiu, P., Chai, F., Curchitser, E.N., Castruccio, F.S., 2018. Future changes in coastal upwelling ecosystems with global warming: the case of the California current System. Nature 8, 2866. https://doi.org/10.1038/s41598-018-21247-7.

Zertuche-González, J., Camacho-Ibar, V., Pacheco-Ruíz, I., Cabello-Pasini, A., Galindo-Bect, L., Guzmán-Calderón, J., Macias-Carranza, V., Espinoza-Avalos, J., 2009. The role of *Ulva* spp. as a temporary nutrient sink in a coastal lagoon with oyster cultivation and upwelling influence. J. Appl. Phycol. https://doi.org/10.1007/s10811-10009-19408-y.